

Boosting the Transferability of Adversarial Attacks with Global Momentum Initialization

Jiafeng Wang^{a,1}, Zhaoyu Chen^{b,c,1}, Kaixun Jiang^{b,c}, Dingkang Yang^{b,c}, Lingyi Hong^a, Pinxue Guo^{b,c}, Haijing Guo^a and Wenqiang Zhang^{a,b,c,*}

^aShanghai Key Lab of Intelligent Information Processing, School of Computer Science, Fudan University, Shanghai 200433, China

^bShanghai Engineering Research Center of AI & Robotics, Academy for Engineering & Technology, Fudan University, Shanghai 200433, China

^cEngineering Research Center of Robotics, Ministry of Education, Academy for Engineering & Technology, Fudan University, Shanghai 200433, China

ARTICLE INFO

Keywords:

Adversarial Examples
Black-box Attacks
Adversarial Transferability
Gradient Optimization
Robustness

ABSTRACT

Deep Neural Networks (DNNs) are vulnerable to adversarial examples, which are crafted by adding human-imperceptible perturbations to the benign inputs. Simultaneously, adversarial examples exhibit transferability across models, enabling practical black-box attacks. However, existing methods are still incapable of achieving the desired transfer attack performance. In this work, focusing on gradient optimization and consistency, we analyse the gradient elimination phenomenon as well as the local momentum optimum dilemma. To tackle these challenges, we introduce Global Momentum Initialization (GI), providing global momentum knowledge to mitigate gradient elimination. Specifically, we perform gradient pre-convergence before the attack and a global search during this stage. GI seamlessly integrates with existing transfer methods, significantly improving the success rate of transfer attacks by an average of 6.4% under various advanced defense mechanisms compared to the state-of-the-art method. Ultimately, GI demonstrates strong transferability in both image and video attack domains. Particularly, when attacking advanced defense methods in the image domain, it achieves an average attack success rate of 95.4%. The code is available at <https://github.com/Omenzychen/Global-Momentum-Initialization>.

1. Introduction

Deep neural networks have shown superior performance in various tasks (He et al., 2016a; Li et al., 2019a; Bojarski et al., 2016; Wang et al., 2018a), but they still exhibit high vulnerability to adversarial examples (Goodfellow et al., 2015; Szegedy et al., 2014; Athalye et al., 2018; Li et al., 2019b), which makes the model lose its original performance by adding some imperceptible perturbations. Moreover, adversarial examples exhibit transferability across models (Wu et al., 2024; Papernot et al., 2017; Huang et al., 2023), meaning adversarial examples crafted to fool one model can deceive other models, making it feasible to perform practical black-box attacks (Kurakin et al., 2018), and the attack process is shown in Figure 1. Hence, gaining a deeper understanding of the generation of adversarial examples with high transferability is essential to enhance model robustness.

Among the existing attack methods, the white-box attack strategy guarantees excellent attack performance by directly obtaining information about the target model but struggles to achieve high transfer attack performance, especially for models with defense mechanisms. To tackle this

challenge, a series of methods have also been proposed to improve transferability for more practical black-box attacks. These methods can be mainly divided into three groups: gradient optimization (Long et al., 2024; Dong et al., 2017; Lin et al., 2020; Wang & He, 2021), data augmentation (Xie et al., 2019; Dong et al., 2019; Wang et al., 2021a), and model augmentation (Liu et al., 2017). Furthermore, in most scenarios, integrating multiple attack methods can lead to improved attack performance.

Considering the aforementioned three attack perspectives, gradient optimization methods tend to be the most commonly used strategy. From the standpoint of optimization, the introduction of momentum (Polyak, 1964) facilitates the accumulation of the attack gradient in the previous direction, achieving higher attack consistency to move the attack direction away from local optima. Most existing optimization methods, such as MI-FGSM (Dong et al., 2017), NI-FGSM (Lin et al., 2020), and VT (Wang & He, 2021), are built upon the momentum. Therefore, we concentrate our analysis on momentum, phenomena of which remain prevalent in most circumstances. Although momentum can improve the effectiveness of attacks, we discover the **gradient elimination** phenomenon still exists during the forward attack process, i.e. the momentum fails to fully converge during the first few iterations leading to inaccurate attack directions, which may inhibit the transferability. Simultaneously, traditional iterative attacks (e.g. MI-FGSM, NI-FGSM) limit the optimization of generated adversarial examples within a very limited data distribution by using a small step size, increasing the likelihood of the attacks converging to local optima. Besides, a direct scaling

*Corresponding author.

Email addresses: jiafengwang21@m.fudan.edu.cn
(Jiafeng Wang); zhaoyuchen20@fudan.edu.cn
(Zhaoyu Chen); kxjiang22@m.fudan.edu.cn
(Kaixun Jiang); dkyang20@fudan.edu.cn (Dingkang Yang); lyhong22@m.fudan.edu.cn (Lingyi Hong); pxguo21@m.fudan.edu.cn (Pinxue Guo); hjguo22@m.fudan.edu.cn (Haijing Guo); wqzhang@fudan.edu.cn (Wenqiang Zhang)

¹Equal contribution.

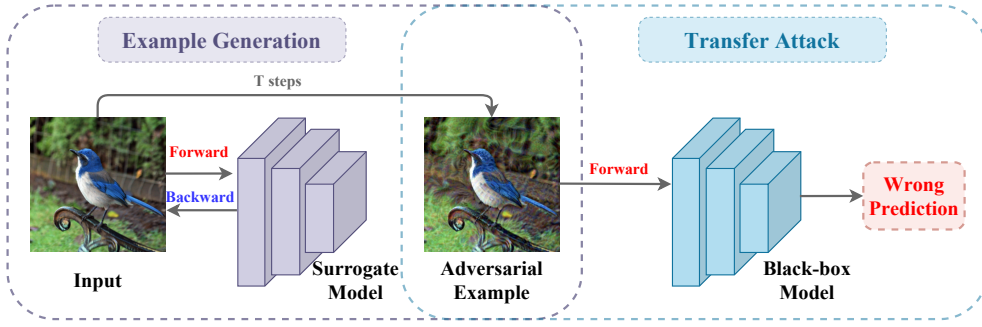


Figure 1. Pipeline of the generation and transfer process of adversarial examples. The module on the left illustrates example generation utilizing the surrogate model for T iterative attacks, while the module on the right delineates the transfer of the generated adversarial examples into the black-box model.

of the step size may cause the attack easily falling into overfitting, as shown in Figure 2a.

To tackle the aforementioned challenges, our study commences by validating the association between gradient consistency and attack efficacy and scrutinizes the phenomenon of gradient elimination. We subsequently propose global momentum initialization to suppress gradient elimination and locate better global optimum over a larger data distribution during pre-convergence. Concretely, we undertake gradient pre-convergence in advance of the attack process to expedite momentum convergence, thus suppressing gradient elimination. Besides, we employ global search in the pre-convergence phase to help the initial momentum converge in a more effective direction. The generated adversarial examples under different methods are shown in Figure 2b. We visualize the attack process in Figure 3 for our method as well as the conventional method. The experimental outcomes demonstrate that our method yields a noteworthy improvement in the attack success rate, even against advanced defense mechanisms, exhibiting a 6.4% increase in success rate over the current state-of-the-art method. Eventually, our approach attains an average attack success rate of 95.4%. In summary, the main contributions are as follows:

- We verify the relationship between gradient consistency and attack performance from both theoretical and experimental perspectives. Based on the proposed gradient consistency, we determine the gradient elimination problem in the current attack methods.

- To suppress gradient elimination, we use pre-convergence as well as global search to improve gradient consistency. Further, we propose Global Momentum Initialization (GI), a novel and efficient attack algorithm, to help the attack find the global optimum.

- Our method can be seamlessly combined with any existing gradient-based attack method. Empirical experiments show that our method can significantly outperform existing state-of-the-art methods across diverse attack settings. Moreover, in addition to the image attack, our method be generalized to video attacks which have higher dimension.

The rest of the paper is organized as follows: In Section 2, we first provide an overview of gradient optimization and input transformation attack strategies, followed by a

brief review of the main defense mechanisms. Section 3 delves into the notion of gradient consistency, based on which we further elucidate the importance of global momentum initialization (a priori momentum knowledge) in improving the efficiency of attacks. We also introduce our new strategy and provide the corresponding algorithmic framework. In Section 4, we present experimental results of black-box attacks in different settings. The experimental results of the attacks are presented for single model, multi-model, advanced defense methods, cross-structure model, and video model. To further analyse our approach, we conduct an ablation study and analyse the experimental results accordingly. Finally, in Section 5, we summarise our study and discuss the impact.

2. Related Work

In this section, we introduce some mainstream attack algorithms from the perspectives of gradient optimization and input transformation. We also provide a brief overview of related advanced defense methods.

2.1. Gradient Optimization Attacks

Fast Gradient Sign Method (FGSM) (Goodfellow et al., 2015). FGSM generates an adversarial example for only one step with the aim of maximizing the loss function:

$$x^{adv} = x^{clean} + \epsilon \cdot \text{sign}(\nabla_x J(x^{clean}, y)),$$

where $\text{sign}(\cdot)$ represents the sign function.

Iterative Fast Gradient Sign Method (I-FGSM) (Kurakin et al., 2018). In contrast to FGSM, I-FGSM divides one iteration into multiple small steps:

$$x_{t+1}^{adv} = x_t^{adv} + \alpha \cdot \text{sign}(\nabla_x J(x_t^{adv}, y)),$$

where $\alpha = \epsilon/T$ is the step size of each attack and T is the number of attack steps.

Momentum Iterative Fast Gradient Sign Method (MI-FGSM) (Dong et al., 2017). Compared with white-box attacks, MI-FGSM integrates the momentum knowledge

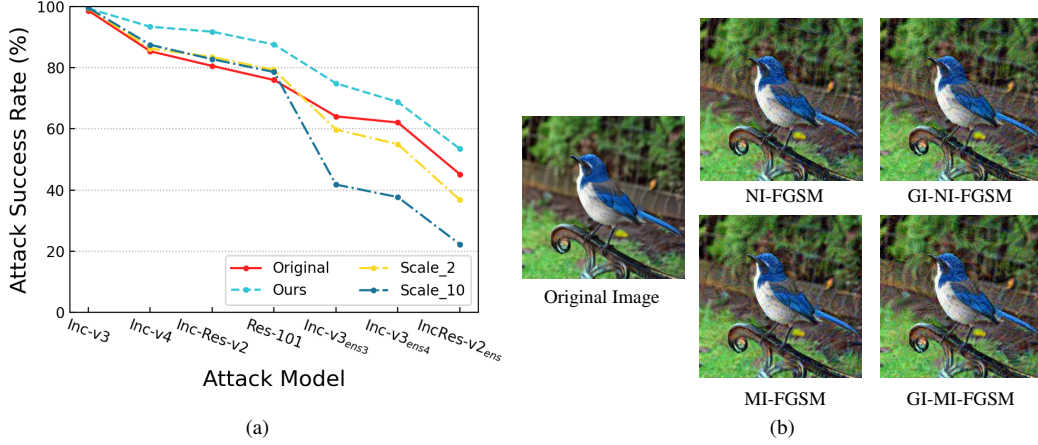


Figure 2. (a) shows the effect of the transfer attack at different step sizes. scale_2 and scale_10 show the results of the attack when the step size is enlarged by two times and ten times, respectively. (b) shows the adversarial examples under different attack methods. All the adversarial examples are generated with Inc-v3.

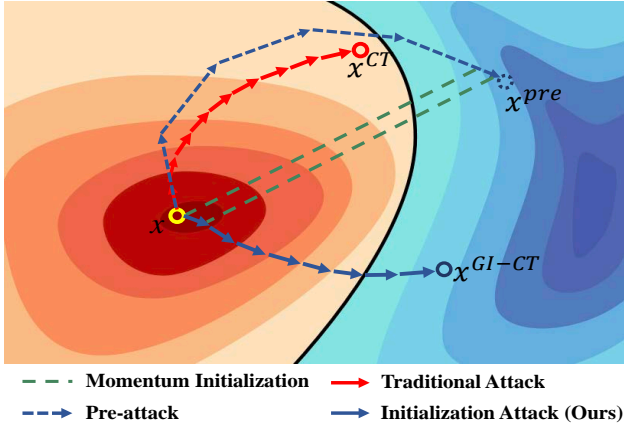


Figure 3. Visualisation of the attack process. CT (Lin et al., 2020) represents the combination of three transformation methods: DIM (Xie et al., 2019), TIM (Dong et al., 2019), SIM (Lin et al., 2020). x represents the original data point and x^{CT} represents the adversarial example obtained under original CT-FGSM. x^{pre} and x^{GI-CT} denote the overall process of the pre-attack as well as the formal attack.

into attack to help the attack direction jump out of the local optimum:

$$g_{t+1} = \mu \cdot g_t + \frac{\nabla_x J(x_t^{adv}, y)}{\|\nabla_x J(x_t^{adv}, y)\|_1}, \quad (1)$$

$$x_{t+1}^{adv} = x_t^{adv} + \alpha \cdot \text{sign}(g_{t+1}),$$

where μ is the decay factor and $g_0 = 0$.

Nesterov Iterative Fast Gradient Sign Method (NI-FGSM) (Lin et al., 2020). NI-FGSM uses Nesterov’s accelerated gradient (Nesterov, 1983) $x_t^{adv} + \alpha \cdot \mu \cdot g_t$ to replace

x_t^{adv} in Eq. (1):

$$g_{t+1} = \mu \cdot g_t + \frac{\nabla_x J(x_t^{adv} + \alpha \cdot \mu \cdot g_t, y)}{\|\nabla_x J(x_t^{adv} + \alpha \cdot \mu \cdot g_t, y)\|_1}, \quad (2)$$

$$x_{t+1}^{adv} = x_t^{adv} + \alpha \cdot \text{sign}(g_{t+1}),$$

This look-ahead process allows attack to move further away from the local optimum, resulting in better attack performance.

Variance Tuning Method (VT) (Wang & He, 2021). VT performs gradient sampling in the domain of data points in each iteration, which allows for the adjustment of the gradient direction with variance knowledge, thereby forming a more accurate and effective attack direction.

Prior optimization methods have primarily focused on identifying a more optimal attack direction, while we present the first theoretical and experimental analysis from the perspective of gradient consistency and identify the gradient elimination issue. To solve the existing issue, we propose global momentum initialization to find a more effective attack direction. We hope that our proposed method can make up for the deficiencies of most of the existing gradient-based attack methods and provide a new optimization perspective for transfer attacks.

2.2. Input Transformations Attacks

Diverse Input Method (DIM) (Xie et al., 2019). DIM performs data augmentation using random scaling and padding operations with a certain probability to alleviate overfitting in adversarial attacks. This strategy provides valuable insights for enhancing transferability.

Translation-Invariant Method (TIM) (Dong et al., 2019). TIM applies convolution transformation of the Gaussian kernel W to the gradient knowledge, resulting in a substantial enhancement of the attack performance, especially

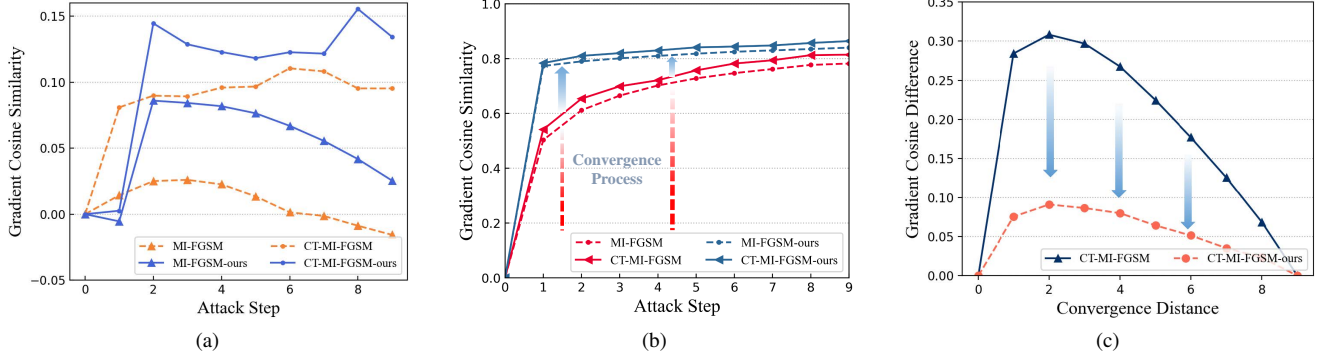


Figure 4. Analysis of gradient consistency (cosine similarity) between iterative attacks. (a) represents the gradient consistency before momentum accumulation; (b) represents the gradient consistency between iterations after momentum accumulation; (c) shows the gradient similarity analysis between the 1st, 10th iteration and other iterations. For instance, when the convergence distance is 2, the gradient consistency between the 1st and 3rd rounds is nearly 0.3 smaller than that between the 10th and 8th rounds. However, with our approach, the difference is less than 0.1. The reduced difference suggests that the degree of consistency between the gradients in the 1st round and those in the other rounds is very similar to the consistency between the gradients in the 10th round and those in the other rounds. This implies a more adequate convergence.

against adversarial-trained models.

$$x_{t+1}^{adv} = x_t^{adv} + \alpha \cdot \text{sign}(W \cdot \nabla_x J(D(x_t^{adv}), y)).$$

Scale-Invariant Method (SIM) (Lin et al., 2020). SIM exploits the scaling invariance of the image and fuses the gradient knowledge of scaled images to improve the transferability. The new optimization objective after scaling is:

$$\text{argmax}_{x^{adv}} \frac{1}{n} \sum_{i=0}^n J(S_i(x^{adv}), y),$$

where scaling factor $S_i(x) = \frac{x}{2^i}$ and n is the scale number.

(Lin et al., 2020) propose Composite Transformation (CT) obtained by combining DIM, TIM, SIM can be one of the most strongest input transformation methods. Our proposed approach, global momentum initialization, can be easily integrated with all input transformation methods.

2.3. Advanced Adversarial Defense

Many defense methods have been proposed in order to suppress the aggressiveness of adversarial examples against neural networks. The mainstream of adversarial defenses is divided into adversarial training as well as adversarial example preprocessing. Adversarial training methods (Goodfellow et al., 2015; Kurakin et al., 2017; Madry et al., 2018) enhance the training data by adversarial examples, thereby refining the model decision boundaries to improve adversarial robustness. The adversarial example preprocessing method focuses on purifying the perturbations of adversarial examples as much as possible by some data enhancement means (Guo et al., 2018; Cohen et al., 2019), e.g. compression or smoothing.

3. Methodology

Given the original image x^{clean} and the corresponding label y , the adversary has to find the perturbation δ to generate adversarial examples x^{adv} to fool the model. To ensure the imperceptibility of the attack, we guarantee $\|x^{clean} - x^{adv}\|_{\infty} \leq \epsilon$. Assume that $f(x^{adv})$ represents the output of the model with input x and the attack is to maximize the loss $J(f(x^{adv}), y)$ (e.g. the cross-entropy loss or margin loss (Carlini & Wagner, 2017)), so the attack goal can be described as:

$$\text{argmax}_{x^{adv}} (J(f(x^{adv}), y)), \quad \text{s.t.} \|x^{clean} - x^{adv}\|_{\infty} \leq \epsilon.$$

3.1. Gradient Elimination

Among the existing gradient optimization methods, MI-FGSM is considered an important baseline. This method improves attack performance by introducing momentum to help accumulate gradients, resulting in more consistent attack directions. Despite the benefits of momentum in enabling the attack to escape from a local optimum, a pertinent question arises as to **whether early gradient attacks may have suboptimal attack performance due to a lack of momentum accumulation, given that momentum accumulation is a time-series process**. Since most optimization-based methods build upon the momentum of MI-FGSM, our analysis revolves around MI-FGSM, and can be extended to other optimization methods such as NI-FGSM. To delve deeper into the aforementioned issue, we leverage **gradient consistency**, i.e., the degree of gradient similarity during the attack, to investigate the correlation between attack gradient and attack optimization objective. We first develop a corollary of the numerical and theoretical relationship among different gradients.

Assuming that the gradient knowledge obtained in the first round of attack is g_1 , then the direction of the first round

of attack is $\text{sign}(g_1)$, and the resulting difference of loss is:

$$\Delta J_1 = J(f(x + \alpha \cdot \text{sign}(g_1)), y) - J(f(x), y). \quad (3)$$

Since the step size α is very small with respect to x , we can treat $\alpha \cdot \text{sign}(g_1)$ as a minimal value, i.e. $\alpha \cdot \text{sign}(g_1) \rightarrow 0$. From the Taylor expansion we can know:

$$f(x + \alpha \cdot \text{sign}(g_1)) = f(x) + \alpha \cdot \text{sign}(g_1) \cdot \frac{\partial f}{\partial x} + O(\alpha^2). \quad (4)$$

For simplicity, we denote $\alpha \cdot \text{sign}(g_1) \cdot \frac{\partial f}{\partial x} + O(\alpha^2)$ as $P(x)$. By substituting Eq. (4) into Eq. (3) and utilizing the Taylor expansion again, we can obtain:

$$\begin{aligned} J(f(x), y) &= J(f(x + \alpha \cdot \text{sign}(g_1)) - P(x), y) \\ &= J(f(x + \alpha \cdot \text{sign}(g_1)), y) \\ &\quad - P(x) \cdot \frac{\partial J}{\partial f} + O(P^2(x)). \end{aligned} \quad (5)$$

Combining Eq. (4) and Eq. (5), since $(g_1 \neq 0)$, we can get:

$$\begin{aligned} \Delta J_1 &= P(x) \cdot \frac{\partial J}{\partial f} = (\alpha \cdot \text{sign}(g_1) \cdot \frac{\partial f}{\partial x} + O(\alpha^2)) \cdot \frac{\partial J}{\partial f} \\ &= \alpha \cdot \text{sign}(g_1) \cdot g_1 \approx \text{sign}(g_1) \cdot \text{sign}(g_1) > 0 \quad (g_1 \neq 0). \end{aligned} \quad (6)$$

Eq. (6) shows that when the first round gradient is attached to the input x , the loss change $\Delta J_1 > 0$, consistent with the fact that the loss increases during the attack process. Similarly, ΔJ_n denotes that if the gradient of the n_{th} iteration is applied to input x , the difference of loss changes to $\Delta J_n \approx \text{sign}(g_1) \cdot \text{sign}(g_n)$. In this context, the input x can be an adversarial example derived from any iteration, so we can test the consistency between gradients of any two rounds to predict the change in loss. In conjunction with the optimization objective, a more effective attack is one that gains greater losses with other rounds. Therefore, to improve attack performance, we should ensure relatively higher gradient consistency.

Based on the above theoretical analysis, we further explore the consistency of gradients under momentum from an experimental perspective. As shown in Figure 4a, the cosine similarity among gradients prior to momentum convergence is nearly zero, meaning that there is a large randomness in attack directions. We argue that the low similarity and high randomness during the attack are the key factors in the overfitting of I-FGSM (Kurakin et al., 2018). On the other hand, Figure 4b illustrates the gradient consistency of different rounds during the attack after the momentum accumulation, and it can be observed that after a few rounds of forward gradient convergence, the gradient consistency rapidly improves and reaches stability. This indicates that the momentum indeed helps the attack gradients reach more common directions, thus improving the attack performance. Simultaneously, when combined with existing data enhancement method CT (Lin et al., 2020), the attack can explore better attack directions with higher attack consistency and attack performance.

However, there still exists inherent flaws in the current methodology. On the one hand, the time-series nature of the

Algorithm 1 Framework of GI-MI-FGSM

Input: A classifier f with fixed parameters θ and loss function J , number of iterations T , maximum perturbation ϵ , input images x , Pre-convergence Iterations P ; Global Search Factor S

Output: An adversarial example x^{adv} ;

```

 $g_0 = 0; x_0^{adv} = x; \alpha = \frac{\epsilon}{T}$ 
for  $t = 0$  to  $P - 1$  do
   $g_{t+1} = \mu \cdot g_t + \frac{\nabla_x J(x_t^{adv}, y)}{\|\nabla_x J(x_t^{adv}, y)\|_1}$ 
   $x_{t+1}^{adv} = \text{Clip}(x_t^{adv} + S \cdot \alpha \cdot \text{sign}(g_{t+1}))$ 
end for
Set global momentum initialization  $g_0 = g_P$ 
for  $t = 0$  to  $T - 1$  do
   $g_{t+1} = \mu \cdot g_t + \frac{\nabla_x J(x_t^{adv}, y)}{\|\nabla_x J(x_t^{adv}, y)\|_1}$ 
   $x_{t+1}^{adv} = \text{Clip}(x_t^{adv} + \alpha \cdot \text{sign}(g_{t+1}))$ 
end for
 $x^{adv} = x_T^{adv}$ 
return  $x^{adv}$ 

```

momentum convergence may lead to different accuracy of the information carried by the momentum at different time series. On the other hand, the accumulation of momentum within a very small data distribution is not conducive to finding a better global momentum and is more susceptible to overfitting. As Figure 4b depicts, although momentum can accelerate the gradient to reach consistency, there remains a convergence process, which to a certain extent inhibits the attack performance improvement. We define this phenomenon where the gradient does not converge enough resulting in a less consistent attack direction as **gradient elimination**.

To fully explore this phenomenon, in addition to exploring neighboring gradient relations, we further investigate gradient consistency relations where there exists the same convergence distance. As shown in Figure 4c, with the same convergence distance guaranteed, the forward unconverged gradient (e.g. the 1st round) is significantly less consistent with the other rounds compared to the backward converged gradient (e.g. the 10th round). This also suggests that the validity of the gradient knowledge is different for different rounds and that the validity is affected by momentum convergence, again confirming the phenomenon of gradient elimination.

3.2. Global Momentum Initialization

To address the challenge of gradient elimination, we introduce a pre-convergence attack strategy aimed at facilitating a more rapid convergence, thereby enhancing the effectiveness of the attack. Furthermore, we incorporate a global search mechanism during the pre-convergence phase to overcome the limitations associated with conventional iterative methods that generate gradients within a confined data distribution.

Specifically, our strategy involves pre-converging the momentum prior to the formal iterative attack, without exerting any substantive impact on the image through this process. We initiate P rounds of momentum exploration, using the obtained momentum knowledge as the initialised momentum. By means of this pre-convergence, we are able to substantially suppress the gradient elimination phenomenon. As shown in Figure 4b and 4c, the consistency of the forward gradient after pre-convergence is substantially improved, and the difference in gradient consistency between the forward unconverged and backward converged gradients and other rounds of gradients is significantly reduced.

Additionally, traditional iterative attacks use a small step size, causing the generated images after each round to be in a similar data distribution. This restricts the attack from exploring decision boundaries over a wider data range, making it more prone to getting stuck in local optimal solutions. (Gao et al., 2020) propose to scale up the step size, but this approach will have a direct impact on the images and easily cause overfitting of the attack. To address this issue, we add a **global search factor** to the pre-convergence process, i.e., we amplify the exploration step size during pre-convergence to help form a more global direction of initialised momentum. Namely, we perform gradient pre-convergence by:

$$g_{t+1} = \mu \cdot g_t + \frac{\nabla_x J(x_t^{adv}, y)}{\|\nabla_x J(x_t^{adv}, y)\|_1},$$

$$x_{t+1}^{adv} = \text{Clip}(x_t^{adv} + S \cdot \alpha \cdot \text{sign}(g_{t+1})),$$

where S represents our global search factor and $\text{Clip}(\cdot)$ operation ensures the l_∞ constraint. The procedure of the attack based on global momentum initialization can be summarised as Algorithm 1.

To further illustrate the efficacy of global momentum initialization in mitigating gradient elimination, we visualize the attack process in Figure 3 for different methods. Since the direction of the attack gets progressively closer to the decision boundary during the optimization, traditional iterative methods may easily suffer from gradient elimination in the forward unconverged attack, i.e., they can only get closer to the decision boundary by a minor distance. For this reason, with the exploration of pre-attack and global momentum initialization, the attack strategy can search for a better attack direction in advance and ensure the consistency of the attack process to successfully cross the decision boundary.

4. Experiment

4.1. Experiment Setup

Dataset. Followed by NIPS’17 Competition (Kurakin et al., 2018), we randomly select 1000 images from the ILSVRC 2012 validation set (Russakovsky et al., 2015), correctly classified and belonging to different categories as our original inputs.

Models. We consider four normally trained models, including Inception-v3 (Inc-v3) (Szegedy et al., 2016), Inception-v4 (Inc-v4) (Szegedy et al., 2017), Inception-Resnet-v2 (IncRes-v2) and Resnet-101 (Res-101) (He et al., 2016b) as well as three adversarially trained models, namely ens3-adv-Inception-v3 (Inc-v3_{ens3}), ens4-adv-Inception-v3 (Inc-v3_{ens4}) and ens-adv-Inception-ResNet-v2 (IncRes-v2_{ens}) (Tramèr et al., 2018). Instead of merely using Inception and ResNet as victim models, we also choose a series of recently popular models such as ViT (Dosovitskiy et al., 2021), Swin-b (Liu et al., 2021), Mixer-mlp (Tolstikhin et al., 2021), DeiT (Touvron et al., 2021), and adversarially trained defense models as victim models. In addition, we adopt nine advanced defense methods to test the attack performance, e.g. HGD (Liao et al., 2018), R&P (Xie et al., 2018), NIPS-r3¹, JPEG (Guo et al., 2018), FD (Liu et al., 2019), ComDefend (Jia et al., 2019), NRP (Naseer et al., 2020), RS (Cohen et al., 2019), Bit-Red (Xu et al., 2018).

Baselines. We follow the standard experimental setting of (Wang & He, 2021; Xie et al., 2019; Wang et al., 2021a). For optimization methods, we regard MI-FGSM (Dong et al., 2017), NI-FGSM (Lin et al., 2020) and the VT (Wang & He, 2021) as our baselines. Simultaneously, for data augmentation methods, we consider DIM (Xie et al., 2019), TIM (Dong et al., 2019), SIM, CT (Lin et al., 2020), i.e., the integrated version of the former three methods. When combining our method with optimization and input transformation methods, we denote final methods as GI-VM(N)I-CT-FGSM, GI-M(N)I-CT-FGSM and GI-M(N)I-FGSM, respectively. Moreover, we have additionally selected several recent state-of-the-art methods as baselines such as SIA (Wang et al., 2023), Admix (Wang et al., 2021a), EMI (Wang et al., 2021b), SSA (Long et al., 2022), PI-FGSM (Gao et al., 2020).

Hyper-parameters. We follow the standard attack settings of (Wang & He, 2021; Xie et al., 2019; Wang et al., 2021a), where we set the maximum perturbation ϵ to 16, the number of iteration rounds T to 10, the iteration step size α to 1, and the decay factor μ to 1 for MI-FGSM and NI-FGSM. As for input transformation methods, we set the transformation probability to 0.5 for DIM. We adopt 7×7 Gaussian kernel for TIM and the scale number for SIM equals 5. For our method, we set pre-convergence iterations P to 5 and global search factor S to 10.

4.2. Attack with Optimization Methods

Initially, we evaluate the performance of our method with the optimization method only, i.e., we combine our method to NI-FGSM and MI-FGSM respectively without considering the input transformation methods. Here we use the attack success rate, the proportion of images misclassified by the attack model as our metric. During the attack, we use four normally trained models as surrogate models to generate adversarial examples iteratively and then transfer

¹<https://github.com/anlhms/nips-2017/tree/master/mmd>

Model	Attack	Inc-v3	Inc-v4	IncRes-v2	Res-101	Inc-v3 _{ens3}	Inc-v3 _{ens4}	IncRes-v2 _{ens}	Avg.
Inc-v3	MI-FGSM	100.0*	44.4	41.5	34.7	14.5	12.4	6.0	36.2
	GI-MI-FGSM	100.0*	54.1	51.9	43.8	14.3	13.4	6.6	40.6
	NI-FGSM	100.0*	52.1	49.9	42.6	13.7	13.9	6.0	39.7
	GI-NI-FGSM	100.0*	58.7	56.0	47.5	13.4	12.0	6.8	42.1
Inc-v4	MI-FGSM	56.3	99.7*	46.7	41.3	16.4	14.8	7.6	40.4
	GI-MI-FGSM	68.6	100.0*	57.0	51.0	16.1	15.8	7.7	45.2
	NI-FGSM	63.3	100.0*	51.1	45.9	15.1	14.4	7.0	42.4
	GI-NI-FGSM	74.7	100.0*	62.4	53.3	16.8	16.2	8.1	47.4
IncRes-v2	MI-FGSM	58.7	50.9	98.1*	45.1	21.6	17.2	11.5	43.3
	GI-MI-FGSM	73.9	64.3	98.5*	57.2	23.0	17.7	12.3	49.6
	NI-FGSM	61.6	54.5	99.1*	45.5	20.1	16.0	9.5	43.8
	GI-NI-FGSM	77.1	68.3	99.5*	58.8	23.8	18.0	11.7	51.0
Res-101	MI-FGSM	58.8	50.8	50.8	99.1*	24.3	22.0	12.9	45.5
	GI-MI-FGSM	71.1	64.6	64.2	99.3*	26.2	21.2	12.4	51.3
	NI-FGSM	64.3	59.4	55.9	99.4*	24.1	21.2	12.3	48.1
	GI-NI-FGSM	74.7	68.6	65.9	99.5*	26.9	21.1	12.0	52.7

Table 1

Attack success rates (%) of seven models using optimization method merely. The adversarial examples are crafted by Inc-v3, Inc-v4, IncRes-v2, Res-101 respectively. * indicates the white box attack setting.

Model	Attack	Inc-v3	Inc-v4	IncRes-v2	Res-101	Inc-v3 _{ens3}	Inc-v3 _{ens4}	IncRes-v2 _{ens}	Avg.
Inc-v3	NI-CT-FGSM	99.5*	84.5	79.0	72.9	57.2	54.8	40.3	69.7
	GI-NI-CT-FGSM	99.8*	93.7	91.0	87.1	70.1	65.9	50.0	79.7
	VNI-CT-FGSM	99.0*	90.1	87.6	84.6	78.6	76.5	66.0	83.2
	GI-VNI-CT-FGSM	99.3*	94.5	92.7	89.7	85.1	83.3	72.9	88.2
	MI-CT-FGSM	98.7*	85.4	80.6	76.0	64.1	62.1	45.2	73.2
	GI-MI-CT-FGSM	99.4*	93.4	91.8	87.6	74.9	68.8	53.5	81.3
	VMI-CT-FGSM	99.0*	88.5	85.7	82.4	77.3	75.9	62.8	81.7
	GI-VMI-CT-FGSM	99.5*	97.1	95.9	92.8	88.0	86.5	74.9	90.7
Inc-v4	NI-CT-FGSM	87.8	99.4*	82.5	75.9	65.8	62.6	51.3	75.0
	GI-NI-CT-FGSM	95.0	99.5*	93.4	87.3	76.7	71.2	59.5	83.2
	VNI-CT-FGSM	92.3	99.7*	89.2	84.9	79.9	77.1	70.5	84.8
	GI-VNI-CT-FGSM	97.6	99.7*	92.6	90.7	88.1	86.2	79.8	90.7
	MI-CT-FGSM	87.2	98.6*	83.3	78.3	72.2	67.2	57.3	77.7
	GI-MI-CT-FGSM	94.5	99.5*	93.2	87.8	77.3	73.8	61.2	83.9
	VMI-CT-FGSM	89.7	98.8*	86.3	82.0	78.1	76.2	67.5	82.7
	GI-VMI-CT-FGSM	97.0	99.8*	95.5	91.7	88.3	86.8	79.4	91.2
IncRes-v2	NI-CT-FGSM	90.2	87.0	99.4*	83.2	75.0	68.9	65.1	81.3
	GI-NI-CT-FGSM	96.0	95.3	99.4*	92.0	84.3	80.7	75.7	89.1
	VNI-CT-FGSM	92.9	90.6	99.0*	88.2	85.2	82.5	81.8	88.6
	GI-VNI-CT-FGSM	96.3	97.3	99.3*	95.4	94.4	91.6	91.0	95.0
	MI-CT-FGSM	88.0	85.5	97.5*	81.6	76.0	71.5	70.2	81.5
	GI-MI-CT-FGSM	95.3	94.7	99.0*	91.4	85.6	82.1	78.4	89.5
	VMI-CT-FGSM	88.9	87.0	97.0*	85.0	83.4	80.5	79.4	85.9
	GI-VMI-CT-FGSM	96.9	96.3	99.4*	94.4	92.6	91.0	89.9	94.4
Res-101	NI-CT-FGSM	86.1	82.2	83.3	98.5*	70.0	68.5	54.6	77.6
	GI-NI-CT-FGSM	94.9	92.7	93.2	99.3*	83.4	78.3	68.7	87.2
	VNI-CT-FGSM	90.7	85.5	87.2	99.1*	82.6	79.7	73.3	85.4
	GI-VNI-CT-FGSM	96.3	95.6	95.5	99.4*	92.4	90.5	85.5	93.6
	MI-CT-FGSM	86.5	81.8	83.2	98.9*	77.0	72.3	61.9	80.2
	GI-MI-CT-FGSM	94.0	92.2	91.8	99.3*	83.9	80.4	70.0	87.4
	VMI-CT-FGSM	86.9	84.2	86.4	98.6*	81.0	78.6	71.6	83.9
	GI-VMI-CT-FGSM	95.8	95.3	94.9	99.3*	92.3	89.8	85.2	93.2

Table 2

Attack success rates (%) of seven black models using both optimization methods and transformation methods. The adversarial examples are crafted by Inc-v3, Inc-v4, IncRes-v2, Res-101 respectively. * indicates the white box attack setting.

them to all models, the results of which are shown in Table 1.

According to the results, we can see that for the four normally trained models, our method improves the black-box attack transferability by a large margin while improving

the white-box performance as well, e.g., for the adversarial examples generated by IncRes-v2 and transferred to Inc-v3, the attack success rate increases from 58.7% and 61.6% to 73.9% and 77.1%, respectively. However, at the same time, we also notice that the improvement for the adversarial-trained models is not as significant as that for

Attack	Inc-v3	Inc-v4	IncRes-v2	Res-101	Inc-v3ens3	Inc-v3ens4	IncRes-v2ens	Average
PI-CT-MI-FGSM	99.4*	82.1	79.8	76.4	57.8	53.1	38.9	69.6
GI-PI-CT-MI-FGSM	99.5*	88.8	85.9	79.2	60.6	56.8	40.7	73.1
SSA-CT-MI-FGSM	99.8*	93.5	92.3	89.4	89.7	88.1	78.5	90.2
GI-SSA-CT-MI-FGSM	100.0*	96.9	96.3	94.2	92.4	91.3	83.2	93.5
Admix-CT-MI-FGSM	99.8*	89.2	86.4	82.7	72.5	67.3	51.5	78.5
GI-Admix-CT-MI-FGSM	100.0*	96.8	94.5	89.0	79.8	74.6	57.0	84.5
EMI-TIDIMI-FGSM	99.6*	86.4	83.0	76.1	53.7	51.0	35.0	69.3
GI-EMI-TIDIMI-FGSM	99.7*	93.7	92.3	85.6	62.4	56.4	40.5	75.8
SIA-MI-FGSM	99.6	90.5	88.6	82.7	75.5	69.5	54.7	80.2
GI-SIA-MI-FGSM	100.0*	96.4	94.9	90.9	85.2	80.1	65.6	87.6

Table 3

Attack success rate (%) of more state-of-the-art methods and the combination with our method. * represents the white-box attack setting. Adversarial examples are generated by Inc-v3.

the normally trained models. We attribute this to the inherent low transferability of the adversarially trained model, which results in the original attack direction not being able to explore a better global optimal direction even after better optimization. This phenomenon will be eliminated when combined with the input transformation methods. Details are available in Section 4.3.

4.3. Attack with State-of-the-art

Further, we verify the performance of GI with both the optimization and input transformation methods. We follow the experimental setup CT in (Lin et al., 2020) and then combine them with the gradient optimization methods: MI-FGSM, NI-FGSM and VT respectively to test the performance. It is crucial to note that the VT entails a non-negligible time and space cost concerning attack performance. To ensure a fair comparison, we test attack performance under both M(N)I-CT-FGSM and VM(N)I-CT-FGSM. The final results are shown in Table 2. In the M(N)I-CT-FGSM condition, our proposed method demonstrates a notable enhancement in the attack success rate, achieving an average improvement of 8.1%. Moreover, our approach achieves a comparable attack performance to the previous state-of-the-art method VM(N)I-CT-FGSM, all the while requiring less than **one-tenth of the time** to execute. In particular, the final method, GI-M(N)I-VT-FGSM, can achieve an average attack success rate of 88.2% ~ 95.0%, which exceeds the previous state-of-the-art method VM(N)I-CT-FGSM by 7.6% in average.

In addition to the previously mentioned baselines, there still exists several popular state-of-the-art methods for enhancing transferability. (Wang et al., 2023) devise the Structure Invariant Attack (SIA), employing various data augmentation techniques to enhance transferability. (Long et al., 2022) propose the use of Spectrum Simulation Attack (SSA) in the frequency domain space to improve attack performance. Admix (Wang et al., 2021a) obtains better gradients for the original image mixed with other images by data enhancement to improve the transferability. EMI (Wang et al., 2021b) is looking ahead with the guidance of local gradient knowledge to get a better attack direction. PI-FGSM (Gao et al., 2020) considers projecting the clipped

Attack	ViT	Swin-b	Mixer-mlp	DeiT	Resnet-101 _{adv}	Swin-b _{adv}	Avg
MI-CT-FGSM	72.0	83.4	82.9	81.8	25.7	20.6	61.1
GI-MI-CT-FGSM	81.9	90.1	92.1	91.0	28.6	21.8	67.6
VMI-CT-FGSM	76.6	85.6	86.8	84.7	28.4	22.7	64.1
GI-VMI-CT-FGSM	87.2	92.3	94.0	94.2	30.9	25.2	70.6

Table 4

Attack success rates (%) under different model architectures. The adversarial examples are crafted by the ensemble of Inc-v3, Inc-v4, IncRes-v2, Res-101 models.

gradient knowledge to make full use of the gradient knowledge to improve attack performance. We also incorporate our method into these state-of-the-art methods to test the performance and the results are shown in Table 3. For EMI, we utilize the official source code provided without the integration of CT. Indeed, in all instances, our approach exhibits a substantial improvement over the existing performance.

Aside from evaluating existing model structures, our experimentation also encompasses popular model frameworks like **ViT**, **DeiT**, **Mixer-mlp**, and **Swin-b**, along with several adversarial-trained models. For details of the experimental outcomes, please refer to Table 4.

4.4. Attack with Ensemble Models

The preceding two subsections have effectively demonstrated the generality and high performance of our approach within the single-source white-box model setting. (Liu et al., 2017) have shown that the adversarial examples generated with the ensemble model are more transferable. We proceed to verify the performance of our approach under the ensemble attack scenario. The results of this evaluation are presented in Table 5. The results indicate that our method yields a significant improvement in the effectiveness of the black-box attack while also enhancing the performance of the white-box attack to some extent under both CT and VT conditions. It is noteworthy that with the ensemble model method, our attack success rate reaches over 98.6% on average, which means that we can basically achieve the performance of white-box attack. Furthermore, under the white-box attack setting, the attack success rate can reach 100% in most circumstances.

Attack	Inc-v3	Inc-v4	Inc-Res-v2	Res-101	Inc-v3 _{ens3}	Inc-v3 _{ens4}	IncRes-v2 _{ens}	Avg.
MI-CT-FGSM	99.4*	99.0*	97.6*	99.7*	91.3	90.1	86.6	94.8
GI-MI-CT-FGSM	100.0*	99.9*	99.8*	100.0*	98.0	97.2	95.0	98.6
NI-CT-FGSM	100.0*	100.0*	99.8*	100.0*	91.8	89.1	84.5	95.0
GI-NI-CT-FGSM	100.0*	99.9*	100.0*	100.0*	98.2	97.4	95.4	98.7
VMI-CT-FGSM	99.7*	99.1*	98.6*	100.0*	93.2	92.3	90.4	96.2
GI-VMI-CT-FGSM	100.0*	100.0*	100.0*	100.0*	98.9	98.6	97.4	99.3
VNI-CT-FGSM	99.7*	99.6*	99.2*	99.9*	94.9	93.8	92.0	97.0
GI-VNI-CT-FGSM	100.0*	100.0*	100.0*	100.0*	98.9	98.5	97.6	99.3

Table 5

Attack success rates (%) of seven models using both optimization methods and input transformation methods. The adversarial examples are crafted by the ensemble of Inc-v3, Inc-v4, IncRes-v2, Res-101 models. * indicates the white box attack setting.

Attack	HGD	R&P	NIPS-r3	JPEG	FD	ComDefend	NRP	RS	Bit-Red	Avg.
MI-CT-FGSM	90.8	88.1	87.6	92.1	88.5	90.4	76.4	69.3	76.4	84.4
GI-MI-CT-FGSM	97.0	95.2	95.8	98.2	95.7	98.1	83.1	78.7	84.3	91.8
NI-CT-FGSM	90.7	86.6	86.5	92.8	89.7	91.3	69.8	64.2	72.2	82.6
GI-NI-CT-FGSM	97.6	95.7	95.9	98.3	95.9	97.3	81.4	78.8	83.8	91.6
VMI-CT-FGSM	92.8	90.4	89.9	93.4	91.2	92.2	83.3	76.9	80.4	87.8
GI-VMI-CT-FGSM	98.5	97.7	97.4	99.0	96.6	98.3	90.3	86.8	89.9	94.9
VNI-CT-FGSM	94.1	92.4	91.6	95.1	92.2	92.3	84.5	77.4	81.4	89.0
GI-VNI-CT-FGSM	98.9	98.1	98.0	99.1	97.8	98.2	90.8	87.2	90.5	95.4

Table 6

Attack success rates (%) of nine advanced defense methods using both optimization methods and transformation methods. The adversarial examples are crafted by the ensemble of Inc-v3, Inc-v4, IncRes-v2, Res-101 models.

4.5. Evaluation on Advanced Defense Methods

To further investigate the performance of our approach under advanced defense methods, we selected several official baselines from the NIPS 2017 competition (Kurakin et al., 2018) for testing, such as HGD (Liao et al., 2018), R&P (Xie et al., 2018), NIPS-r3, along with several classical methods for adversarial defense, such as JPEG (Guo et al., 2018), FD (Liu et al., 2019), ComDefend (Jia et al., 2019), NRP (Naseer et al., 2020), RS (Cohen et al., 2019), Bit-Red (Xu et al., 2018), to further test the performance of attacks under defense conditions. Here we test the attack performance with the integrated model and the single model (Inc-v3) respectively. The attack results for the integrated model are shown in Table 6.

The results are impressive in that our attack method achieves an average attack success rate of 91.6% ~ 95.4%, outperforming the previous VM(N)I-CT-FGSM method by 6.4% ~ 9.0%, which also indicates the vulnerability and fragility of the existing defense methods.

4.6. Attack with Video Models

To verify the generality of our method, we further validate the experimental performance in video recognition attacks. Following the experimental setup of (Wei et al., 2022), we choose UCF-101 (Soomro et al., 2012) for the dataset, NL (Wang et al., 2018b), SlowFast (Feichtenhofer et al., 2019) and TPN (Yang et al., 2020) for the video recognition models, and Resnet-50 and Resnet-101 are chosen as the backbone for each network, respectively.

We conduct experiments under TT (Wei et al., 2022), a powerful baseline for transfer attacks against video recognition models, FGSM (Goodfellow et al., 2015), and the proposed method (GI) in this section, respectively. Following the standard experimental setup of (Wei et al., 2022), we set the number of iterations $T = 1$ and the maximum perturbation $\epsilon = 16$. The experimental results are shown in Table 7, which shows that the proposed method in this section is also extremely effective in attacking the video recognition model, and can improve the success rate of the transfer attack by more than 15% on average. Overall, this section confirms the effectiveness of the proposed method in video recognition attacks, and also fully illustrates the generalization and effectiveness of the proposed method in attacks in different domains.

4.7. Ablation Study

In this section, we conduct a series of ablation experiments on the hyperparameters. We consider Inc-v3 to generate adversarial examples under the CT method and transfer them to all models, and then do separate ablation experiments on pre-convergences as well as the search amplification factor. All experimental hyperparameters of the other methods are kept constant. **Pre-convergence Iterations P** . Given the sequential necessity of both pre-convergence and global search, we first explore the effect of pre-convergence rounds P on the attack results. As the experimental results in Figure 5a, 5b demonstrate, we can find that just one step of pre-convergence yields a certain performance improvement that increases gradually with incremental P until it stabilizes. This is a strong indication that there is gradient

Model	Attack	NL-Res101	NL-Res50	SlowFast-Res101	SlowFast-Res50	TPN-Res101	TPN-Res50	Avg.
NL-Res101	FGSM	77.2*	84.2	37.6	46.5	13.9	21.8	46.9
	GI-FGSM	100.0*	91.3	34.6	49.3	15.8	18.8	51.6
	TT	72.3*	72.3	49.5	57.4	30.7	44.5	54.5
	GI-TT-FGSM	99.0*	87.8	61.3	69.3	43.3	57.9	69.7
SlowFast-Res101	FGSM	42.6	58.4	79.2*	63.4	28.7	38.6	51.8
	GI-FGSM	41.5	57.6	99.0*	81.9	29.7	39.6	58.2
	TT	58.4	65.3	71.3*	58.4	29.7	41.6	54.1
	GI-TT-FGSM	77.4	82.1	98.0*	81.1	40.5	60.4	73.3
TPN-Res101	FGSM	57.4	67.3	49.5	46.5	36.6*	47.5	50.8
	GI-FGSM	68.7	76.4	45.5	50.8	88.1*	59.6	64.8
	TT	55.5	65.3	47.5	47.5	46.5*	52.5	52.5
	GI-TT-FGSM	68.3	79.8	52.4	53.4	96.0*	67.3	69.5

Table 7

Attack success rates (%) under video models. The adversarial examples are crafted by NL-Res101, SlowFast-Res101, TPN-Res101 models respectively. * indicates the white box attack setting.

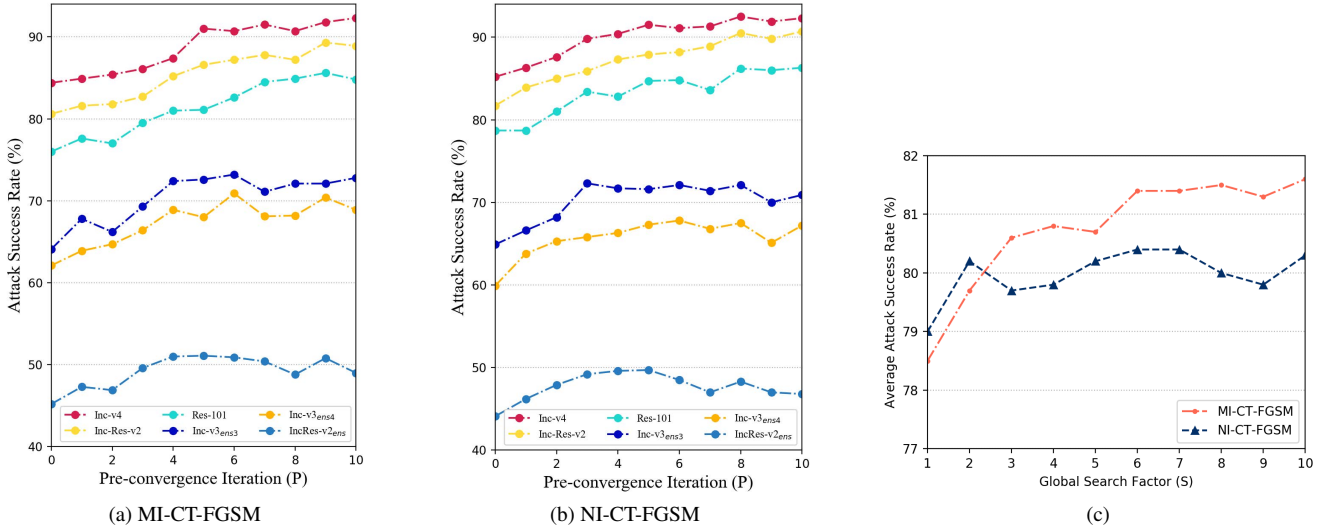


Figure 5. Ablation experiments on pre-convergence and global search factors. (a) and (b) represent attack success rate for six black box models using different pre-convergence iterations. (c) represents the average attack success rate of six models with different global search factors.

elimination in the unpreconverged gradient, and that pre-convergence suppresses this phenomenon, thus improving attack performance. Finally, we choose $P = 5$ to balance the success rate of the attack with the time taken by the attack.

Global Search Factor S . After determining the number of pre-convergence iterations, we further investigate the effect of the global search factor at $P = 5$, the results are shown in Figure 5c. It can be seen that the attack performance improves significantly with the increase of the amplification factor and gradually stabilizes, which illustrates that the global search helps the momentum to find a better global optimal solution. In the end, we choose $S = 10$.

For the sake of ensuring a fair comparison, we evaluate our method against a baseline that employs a strategy of employing a large step size during the initial P steps and subsequently transitioning to a smaller step size for the subsequent T steps. The results are shown in Table 8. It can be seen that without our momentum initialization, even with a guaranteed higher number of iteration rounds, the attack success rate can only reach 68.1%, while corresponding to our method we can achieve an attack success rate of 81.3%. The absence of performance improvement when

simply adding extra iteration rounds further highlights the significance of momentum initialization. We posit that the direct attack approach fails due to two main reasons. Firstly, the usage of an excessively large step size results in overfitting of the attack, as elaborated in detail in Table 2a. Secondly, the issue of gradient elimination remains unresolved, trapping the attack in a locally optimal solution due to the unconverged direction of the attack.

5. Conclusion

In this paper, we present an analysis of the limitations of existing optimization methods from the viewpoint of gradient consistency. We identify the issue of gradient elimination, which may hinder the effectiveness of forward attack attempts. Additionally, we observe that traditional iterative attacks rely on smaller steps that restrict the attack within a limited data distribution, leading to a higher probability of being trapped in a local optimum. Our proposal is to address these issues by global momentum initialization in the form of high-step size pre-convergence, which provides high-quality momentum knowledge for the attack during

Attack	Inc-v3	Inc-v4	IncRes-v2	Res-101	Inc-v3 _{ens3}	Inc-v3 _{ens4}	IncRes-v2 _{ens}	Avg-
MI-CT-FGSM	99.3*	85.8	84.1	87.5	48.0	43.5	28.1	68.1
GI-MI-CT-FGSM	99.4*	93.4	91.8	87.6	74.9	68.8	53.5	81.3

Table 8

Attack success rate (%) of MI-CT-FGSM and the combination with our method. Here the MI-CT-FGSM employs the same $P + T$ attack iterations to guarantee the same attack time as the our GI-MI-CT-FGSM. Adversarial examples are generated by Inc-v3.

the initial stage, suppressing gradient elimination and enhancing its performance significantly. Our approach can be combined with almost all gradient-based optimization methods. Empirical experiments demonstrate that our method achieves an average success rate of 95.4% with the nine existing advanced defense methods, significantly exceeding the previous state-of-the-art success rate of 89.0%. Further, our method also shows impressive performance in video attacks. We hope our method can serve as a new baseline to validate the effectiveness of existing defense methods in the future.

Limitation. Most of the current transfer attack methods suffer from a significant drop in performance when under cross-model structure, and our method does not address this issue well. On the other hand, the current proposed method has only been validated in classification tasks, and its performance should be explored under more tasks.

Future Work. Although GI-FGSM has been shown to be very effective in improving transferability, we believe there are still several aspects that deserve further exploration in the future. From a task perspective, GI-FGSM is currently only applicable to classification tasks, and the performance of the method under other tasks can be explored. From the attack process of the algorithm, further optimization of the algorithm can be considered by adding the pre-convergence process to the iterative attack to reduce the time cost. From a theoretical point of view, gradient consistency can be utilized to explore the generation of generalized perturbations.

CRedit authorship contribution statement

Jiafeng Wang: Conceptualization, Investigation, Experimentation, Visualization, Writing-Original Draft, Review & Editing. Zhaoyu Chen: Supervision, Experimentation, Writing-Original Draft, Review & Editing. Kaixun Jiang: Investigation, Experimentation, Review & Editing. Dingkan Yang: Investigation, Review & Editing. Lingyi Hong: Investigation, Review & Editing. Pinxue Guo: Review & Editing. Haijing Guo: Review & Editing. Wenqiang Zhang: Supervision, Review & Editing, Funding acquisition.

Declaration of competing interest

The authors declare that they have no known competing financial interests or personal relationships that could have appeared to influence the work reported in this paper.

Data availability

Data will be made available on request.

Acknowledgments

This work was supported by National Natural Science Foundation of China (No.62072112), Scientific and Technological innovation action plan of Shanghai Science and Technology Committee (No.22511102202), Fudan Double First-class Construction Fund (No. XM03211178).

References

- Athalye, A., Carlini, N., & Wagner, D. A.(2018). Obfuscated gradients give a false sense of security: Circumventing defenses to adversarial examples. In J. G. Dy, & A. Krause (Eds.), *ICML* (pp. 274–283). PMLR volume 80.
- Bojarski, M., Del Testa, D., Dworakowski, D., Firner, B., Flepp, B., Goyal, P., Jackel, L. D., Monfort, M., Muller, U., Zhang, J. et al.(2016). End to end learning for self-driving cars. *arXiv preprint arXiv:1604.07316*.
- Carlini, N., & Wagner, D. A.(2017). Towards evaluating the robustness of neural networks. In *IEEE Symposium on Security and Privacy* (pp. 39–57).
- Cohen, J. M., Rosenfeld, E., & Kolter, J. Z.(2019). Certified adversarial robustness via randomized smoothing. In K. Chaudhuri, & R. Salakhutdinov (Eds.), *ICML* (pp. 1310–1320). volume 97.
- Dong, Y., Liao, F., Pang, T., Hu, X., & Zhu, J.(2017). Discovering adversarial examples with momentum. *arXiv preprint arXiv:1710.06081*.
- Dong, Y., Pang, T., Su, H., & Zhu, J.(2019). Evading defenses to transferable adversarial examples by translation-invariant attacks. In *CVPR* (pp. 4312–4321).
- Dosovitskiy, A., Beyer, L., Kolesnikov, A., Weissenborn, D., Zhai, X., Unterthiner, T., Dehghani, M., Minderer, M., Heigold, G., Gelly, S., Uszkoreit, J., & Houlsby, N.(2021). An image is worth 16x16 words: Transformers for image recognition at scale. In *ICLR*.
- Feichtenhofer, C., Fan, H., Malik, J., & He, K.(2019). Slowfast networks for video recognition. In *ICCV* (pp. 6202–6211).
- Gao, L., Zhang, Q., Song, J., Liu, X., & Shen, H. T.(2020). Patch-wise attack for fooling deep neural network. In *ECCV* (pp. 307–322). Springer.
- Goodfellow, I. J., Shlens, J., & Szegedy, C.(2015). Explaining and harnessing adversarial examples. In *ICLR*.
- Guo, C., Rana, M., Cissé, M., & van der Maaten, L.(2018). Countering adversarial images using input transformations. In *ICLR*.
- He, K., Zhang, X., Ren, S., & Sun, J.(2016a). Deep residual learning for image recognition. In *CVPR* (pp. 770–778).
- He, K., Zhang, X., Ren, S., & Sun, J.(2016b). Identity mappings in deep residual networks. In B. Leibe, J. Matas, N. Sebe, & M. Welling (Eds.), *ECCV* (pp. 630–645). Springer volume 9908 of *Lecture Notes in Computer Science*.

- Huang, H., Chen, Z., Chen, H., Wang, Y., & Zhang, K.(2023). T-SEA: transfer-based self-ensemble attack on object detection. In *CVPR* (pp. 20514–20523).
- Jia, X., Wei, X., Cao, X., & Foroosh, H.(2019). Comdefend: An efficient image compression model to defend adversarial examples. In *CVPR* (pp. 6084–6092).
- Kurakin, A., Goodfellow, I. J., & Bengio, S.(2017). Adversarial machine learning at scale. In *ICLR*.
- Kurakin, A., Goodfellow, I. J., & Bengio, S.(2018). Adversarial examples in the physical world. In *Artificial intelligence safety and security* (pp. 99–112). Chapman and Hall/CRC.
- Li, X., Gao, L., Wang, X., Liu, W., Xu, X., Shen, H. T., & Song, J.(2019a). Learnable aggregating net with diversity learning for video question answering. In *ACM MM* (pp. 1166–1174).
- Li, Y., Li, L., Wang, L., Zhang, T., & Gong, B.(2019b). NATTACK: learning the distributions of adversarial examples for an improved black-box attack on deep neural networks. In K. Chaudhuri, & R. Salakhutdinov (Eds.), *ICML* (pp. 3866–3876). volume 97.
- Liao, F., Liang, M., Dong, Y., Pang, T., Hu, X., & Zhu, J.(2018). Defense against adversarial attacks using high-level representation guided denoiser. In *CVPR* (pp. 1778–1787).
- Lin, J., Song, C., He, K., Wang, L., & Hopcroft, J. E.(2020). Nesterov accelerated gradient and scale invariance for adversarial attacks. In *ICLR*.
- Liu, Y., Chen, X., Liu, C., & Song, D.(2017). Delving into transferable adversarial examples and black-box attacks. In *ICLR*.
- Liu, Z., Lin, Y., Cao, Y., Hu, H., Wei, Y., Zhang, Z., Lin, S., & Guo, B.(2021). Swin transformer: Hierarchical vision transformer using shifted windows. In *ICCV* (pp. 9992–10002).
- Liu, Z., Liu, Q., Liu, T., Xu, N., Lin, X., Wang, Y., & Wen, W.(2019). Feature distillation: Dnn-oriented jpeg compression against adversarial examples. In *CVPR* (pp. 860–868).
- Long, S., Tao, W., Li, S., Lei, J., & Zhang, J.(2024). On the convergence of an adaptive momentum method for adversarial attacks. *AAAI*, 38, 14132–14140.
- Long, Y., Zhang, Q., Zeng, B., Gao, L., Liu, X., Zhang, J., & Song, J.(2022). Frequency domain model augmentation for adversarial attack. In *ECCV* (pp. 549–566). Springer.
- Madry, A., Makelov, A., Schmidt, L., Tsipras, D., & Vladu, A.(2018). Towards deep learning models resistant to adversarial attacks. In *ICLR*.
- Naseer, M., Khan, S. H., Hayat, M., Khan, F. S., & Porikli, F.(2020). A self-supervised approach for adversarial robustness. In *CVPR* (pp. 259–268).
- Nesterov, Y.(1983). A method for unconstrained convex minimization problem with the rate of convergence $O(1/k^2)$. In *Doklady an ussr* (pp. 543–547). volume 269.
- Papernot, N., McDaniel, P. D., Goodfellow, I. J., Jha, S., Celik, Z. B., & Swami, A.(2017). Practical black-box attacks against machine learning. In R. Karri, O. Sinanoglu, A. Sadeghi, & X. Yi (Eds.), *AsiaCCS* (pp. 506–519). ACM.
- Polyak, B. T.(1964). Some methods of speeding up the convergence of iteration methods. *Ussr computational mathematics and mathematical physics*, 4, 1–17.
- Russakovsky, O., Deng, J., Su, H., Krause, J., Satheesh, S., Ma, S., Huang, Z., Karpathy, A., Khosla, A., Bernstein, M. S., Berg, A. C., & Li, F.(2015). Imagenet large scale visual recognition challenge. *Int. J. Comput. Vis.*, 115, 211–252.
- Soomro, K., Zamir, A. R., & Shah, M.(2012). Ucf101: A dataset of 101 human actions classes from videos in the wild. *arXiv preprint arXiv:1212.0402*, .
- Szegedy, C., Ioffe, S., Vanhoucke, V., & Alemi, A.(2017). Inception-v4, inception-resnet and the impact of residual connections on learning. In *AAAI*. volume 31.
- Szegedy, C., Vanhoucke, V., Ioffe, S., Shlens, J., & Wojna, Z.(2016). Rethinking the inception architecture for computer vision. In *CVPR* (pp. 2818–2826).
- Szegedy, C., Zaremba, W., Sutskever, I., Bruna, J., Erhan, D., Goodfellow, I. J., & Fergus, R.(2014). Intriguing properties of neural networks. In *ICLR*.
- Tolstikhin, I. O., Houlsby, N., Kolesnikov, A., Beyer, L., Zhai, X., Unterthiner, T., Yung, J., Steiner, A., Keysers, D., Uszkoreit, J., Lucic, M., & Dosovitskiy, A.(2021). Mlp-mixer: An all-mlp architecture for vision. In M. Ranzato, A. Beygelzimer, Y. N. Dauphin, P. Liang, & J. W. Vaughan (Eds.), *NeurIPS* (pp. 24261–24272).
- Touvron, H., Cord, M., Douze, M., Massa, F., Sablayrolles, A., & Jégou, H.(2021). Training data-efficient image transformers & distillation through attention. In *ICML* (pp. 10347–10357).
- Tramèr, F., Kurakin, A., Papernot, N., Goodfellow, I. J., Boneh, D., & McDaniel, P. D.(2018). Ensemble adversarial training: Attacks and defenses. In *ICLR*.
- Wang, H., Wang, Y., Zhou, Z., Ji, X., Gong, D., Zhou, J., Li, Z., & Liu, W.(2018a). Cosface: Large margin cosine loss for deep face recognition. In *CVPR* (pp. 5265–5274).
- Wang, X., Girshick, R., Gupta, A., & He, K.(2018b). Non-local neural networks. In *CVPR* (pp. 7794–7803).
- Wang, X., & He, K.(2021). Enhancing the transferability of adversarial attacks through variance tuning. In *CVPR* (pp. 1924–1933).
- Wang, X., He, X., Wang, J., & He, K.(2021a). Admix: Enhancing the transferability of adversarial attacks. In *ICCV* (pp. 16158–16167).
- Wang, X., Lin, J., Hu, H., Wang, J., & He, K.(2021b). Boosting adversarial transferability through enhanced momentum. In *BMVC* (p. 272).
- Wang, X., Zhang, Z., & Zhang, J.(2023). Structure invariant transformation for better adversarial transferability. In *ICCV* (pp. 4607–4619).
- Wei, Z., Chen, J., Wu, Z., & Jiang, Y.-G.(2022). Boosting the transferability of video adversarial examples via temporal translation. In *AAAI* (pp. 2659–2667). volume 36.
- Wu, S., Tan, Y.-a., Wang, Y., Ma, R., Ma, W., & Li, Y.(2024). Towards transferable adversarial attacks with centralized perturbation. *AAAI*, 38, 6109–6116.
- Xie, C., Wang, J., Zhang, Z., Ren, Z., & Yuille, A. L.(2018). Mitigating adversarial effects through randomization. In *ICLR*.
- Xie, C., Zhang, Z., Zhou, Y., Bai, S., Wang, J., Ren, Z., & Yuille, A. L.(2019). Improving transferability of adversarial examples with input diversity. In *CVPR* (pp. 2730–2739).
- Xu, W., Evans, D., & Qi, Y.(2018). Feature squeezing: Detecting adversarial examples in deep neural networks. In *NDSS*.
- Yang, C., Xu, Y., Shi, J., Dai, B., & Zhou, B.(2020). Temporal pyramid network for action recognition. In *CVPR* (pp. 591–600).